

Observation of a precursor in the adsorption of molecular oxygen on Si(100) 2×1G. Comtet,^{1,2} K. Bobrov,^{2,*} L. Hellner,^{1,2} and G. Dujardin^{1,2}¹*Laboratoire pour l'Utilisation du Rayonnement Electromagnétique (LURE), Bât. 209 D, Centre Universitaire Paris-Sud, BP 34, 91898 Orsay Cedex, France*²*Laboratoire de Photophysique Moléculaire, Bât. 210, Université de Paris-Sud, 91405 Orsay Cedex, France*

(Received 29 July 2002; revised manuscript received 20 November 2003; published 16 April 2004)

Molecular oxygen adsorption on the Si(100) 2×1 surface has been studied at low and room temperatures by combining ultraviolet photoemission spectroscopy and photon stimulated desorption (PSD) of ions near the Si (2*p*) excitation edge. PSD studies as a function of oxygen exposure and photon energy have revealed an oxygen precursor on the Si(100) 2×1 surface. This precursor has been observed only at low temperature (50 K) and very low oxygen exposures (<0.06 L). It consists in a molecular or atomic species bonded to a Si surface atom in a top position.

DOI: 10.1103/PhysRevB.69.155315

PACS number(s): 68.43.-h, 68.43.Tj, 73.90.+f

I. INTRODUCTION

Oxidation of silicon is a vitally important process in microelectronic manufacturing. The crucial point of future electronics is the thickness of the insulating SiO₂ layer which forms the basis of field effect transistors (FET).^{1,2} It is now possible to fabricate FET devices with a SiO₂ gate thickness of 1.3 nm (Ref. 3), which corresponds to about ten silicon atoms across the Si/SiO₂ interface. The limit for the insulating layer thickness is determined by the presence of the silicon suboxides in the Si/SiO₂ interface. These oxygen-deficient suboxides are significantly more conductive than the insulating SiO₂, and cause an electrical shortage when the overall thickness is reduced down to a certain limit (1.2 nm, as found by Muller *et al.*²). Therefore, oxygen adsorption, which reveals various silicon suboxides SiO_x ($x = 0-2$) on the silicon surface and represents the initial stage of the Si/SiO₂ interface formation, is a process of great importance which has been intensively studied both theoretically⁴⁻⁶ and experimentally⁷⁻¹² during the last years. However, there are several aspects of oxygen adsorption which are still not clear. One of them is whether an oxygen precursor state exists under initial molecular oxygen adsorption on the clean silicon Si(100) 2×1 surface. Molecular beam studies⁸ suggest the existence of a precursor although this has not been confirmed experimentally. The bonding configurations and electronic structures of the oxygenated species after the initial oxygen adsorption have been studied theoretically only.^{4,5} We emphasize here that a knowledge of these bonding configurations during the initial steps of oxygen adsorption is an important prerequisite for the kinetic Monte Carlo investigations of silicon oxidation.^{13,14}

Oxygen adsorption at low temperatures, at which the precursor is most likely to be observed, has been previously investigated by Sylvestre and Shayegan¹⁵ and Seo *et al.*¹⁶ From work-function measurements of the Si(100) 2×1 surface exposed to oxygen, an electronegative species has been detected at low temperature.^{15,16} Ultraviolet photoemission spectroscopy (UPS) measurements have evidenced broad states below the Fermi level at low temperature which are not visible at room temperature.¹⁶ Seo *et al.*¹⁶ concluded that an O₂ molecular precursor exists on the Si(100) 2×1 sur-

face at 40 K. However the work-function measurement does not allow an unambiguous assignment of the electronegative species. Moreover, the photoemission bands located near the Fermi level can be associated with various oxygen adsorption configurations, and not exclusively to an oxygen molecule on top position. More importantly, the work function measurement is sensitive to rather high oxygen exposures, of the order of 1 L. Actually, the search for a precursor requires a more sensitive technique, such as the photon stimulated desorption (PSD) of ions, able to probe the oxygen adsorption in a much lower oxygen exposure range, of the order of 0.1 L. In this paper, we present a study of the initial molecular oxygen adsorption on the clean Si(100) 2×1 surface at low and room temperatures by UPS and PSD of O⁺ ions near the Si (2*p*) excitation edge. The O⁺ ion desorption clearly evidences that, at very low oxygen exposures, O₂ molecules adsorb differently at 50 and 300 K. At 50 K, O₂ molecules adsorb with at least one oxygen atom on top of a Si atom, while at 300 K both O atoms of the O₂ molecule are in the Si back bonds. This low temperature precursor has been observed only at oxygen exposures smaller than 0.06 L, thus confirming that the observation of the precursor requires a very sensitive surface technique such as the photon stimulated ion desorption, which has been used here.

II. EXPERIMENT

Experiments have been performed *in situ* in an ultrahigh vacuum (UHV) chamber with a base pressure of 2×10^{-11} Torr. The UHV chamber was equipped with a hemispherical electrostatic analyzer and a quadrupole ion spectrometer. The dispersed synchrotron radiation from SuperACO (Orsay storage ring) has been used as a linearly polarized photon source of variable energy in the 30–150-eV range.

The silicon sample [*p*-type Si(100), $\rho = 1 \Omega \text{ cm}$] of $25 \times 6 \times 0.25\text{-mm}^3$ size was mounted on a specially designed sample holder which allowed to vary the detection angle of electrons and ions emitted from the surface and to control the surface temperature in a wide temperature range. The sample holder enabled are (i) to cool the sample down to 50 K by using a liquid helium flow cryostat, and (ii) to heat the

sample up to 1500 K by direct resistive heating. In the former case, the temperature was measured by a chromel-alumel thermocouple attached to the holder in a close vicinity to the sample. In the latter case, the temperature was controlled by an infrared pyrometer.

The clean silicon surface was prepared as follows. First, the sample was outgassed for at least 12 h by resistive heating at 700 °C. In order to remove the oxide layer, the sample was flashed at 1040 °C for 30 sec. Then the sample was cooled down rapidly to 700 °C and then gradually to room temperature. If necessary, the flashing procedure was repeated two or three times. The pressure in the UHV chamber during the flash did not exceed 5×10^{-10} mbar.

Molecular oxygen adsorption was done *in situ* on the clean Si(100) 2×1 surface in the 50–350 K temperature range. During the adsorption, the UHV chamber was back-filled with oxygen at $P = 1 \times 10^{-9}$ to 5×10^{-9} mbar for 1–30 min depending on the exposure. The adsorption doses were calculated by multiplying the pressure by the exposure time ($1 \text{ L} \equiv 10^{-6}$ Torr sec).

All the measurements have been performed at the same temperature as the oxygen adsorption. The synchrotron radiation was used in the three following modes. First, a monochromatized synchrotron light of fixed energy ($h\nu = 120$ eV) was used as an excitation source to stimulate O^+ ion desorption and to monitor the kinetics of oxygen adsorption on the silicon surface as a function of the oxygen exposure. Second, we used the synchrotron radiation as a monochromatic light source of variable energy ($h\nu = 90\text{--}130$ eV) to study O^+ photodesorption from the preadsorbed silicon surfaces near the Si ($2p$) excitation edge. In both modes, photodesorbed O^+ ions were always collected along the normal to the surface. Third, the synchrotron radiation was used as a monochromatic light source of variable energy ($h\nu = 45\text{--}55$ eV) to study the valence-band electron photoemission of oxygen adsorbed on the silicon surface.

The kinetics of oxygen adsorption on the clean Si(100) 2×1 surface (mode I) was studied by monitoring the intensity of photodesorbed O^+ ions during the oxygen exposure. The rate of the O^+ ion photodesorption was found to be low enough compared with the adsorption rate so that this O^+ photodesorption did not affect the oxygen adsorption kinetics. Only O^+ desorbed ions (accompanied by F^+ traces) were detected by the quadrupole ion detector. Photon-stimulated desorption spectra of O^+ ions as a function of the photon energy (mode II) were recorded *after* oxygen adsorption, i.e., once a certain oxygen coverage had been achieved. Valence band photoemission spectra (mode III) were recorded for various photon energies in the 45–55 eV range. The linear polarization of the photon beam was in a plane perpendicular to the surface. The kinetic energy distribution of emitted electrons was analyzed by the electron analyzer in a direction perpendicular to the photon beam. Thus, the incident (θ_i) and emission (θ_e) angles were linked by the $\theta_e = 90 - \theta_i$ relation, and can be adjusted by rotating the sample around its vertical axis. The actual values of the photon energy and emission angle were chosen to obtain the maximum sensitivity of the oxygen-induced bands in the photoemission spectra.

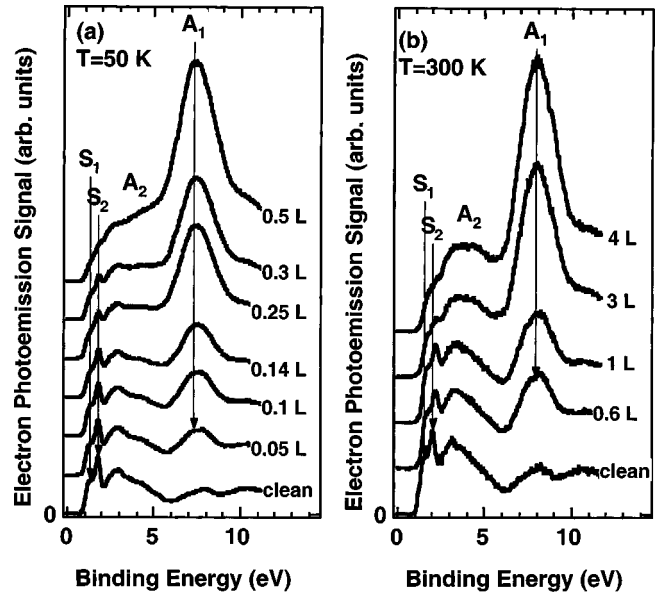


FIG. 1. Electron photoemission spectra of the clean Si(100) 2×1 surface as a function of oxygen exposure at (a) 50 K and (b) 300 K. The photon energy is 55 eV.

III. RESULTS AND DISCUSSION

Our combined electron photoemission and ion photodesorption studies of the oxidation of the Si(100) 2×1 surface have been concentrated on low oxygen exposure ranges similar to the ones used in previous scanning tunneling microscopy (STM) experiments.^{17–19} Many other experimental results^{7–12,20} are associated with higher oxygen exposures. STM experiments^{17–19} have been performed only at room temperature while our experiments have been performed both at low and room temperatures, so that we can expect to have a new insight in the adsorption process. As a matter of fact, due to the high sensitivity of the ion desorption technique, the temperature change has revealed the presence of an adsorption configuration at 50 K, which is not present at 300 K.

A. Ultraviolet photoemission spectroscopy

Electron photoemission spectra of the clean silicon Si(100)- 2×1 surface as a function of oxygen exposure at 50 and 300 K are shown in Figs. 1(a) and 1(b), respectively. The S_1 and S_2 photoemission bands, appearing on the clean surface at binding energies of 0.9 and 1.3 eV, represent the surface states of the silicon dimers.²¹ After oxygen exposure, two broad bands appear. The A_1 band, centered at a binding energy of ~ 7.3 eV, has been previously observed on both oxygen adsorbed Si(100) and Si(111) surfaces.²² The A_2 band is less intense and centered at 2–5 eV. The A_2 band relative to the A_1 band is more intense at low temperature than at room temperature (see Fig. 1). This corroborates the observation by Seo *et al.*¹⁶ of the A_2 band only at low temperature. Photoemission spectra have been recorded for different photon energies ranging from 40 up to 60 eV and the A_2 band could not be resolved in different bands as it was the case for O_2 on Si(111) 7×7 (Ref. 23). Considering the re-

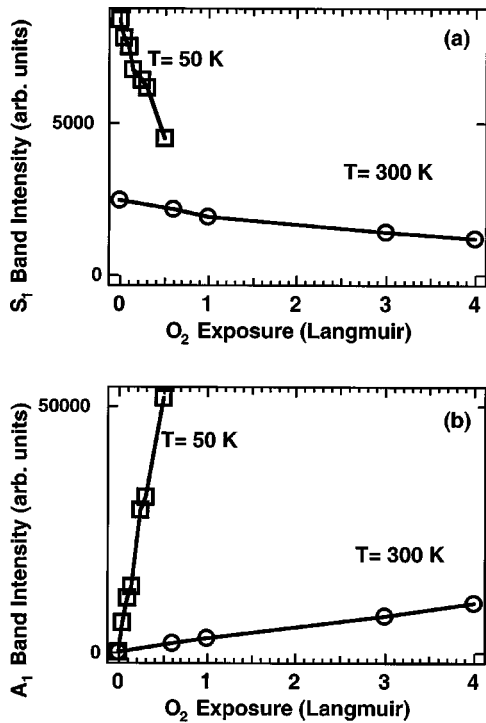


FIG. 2. Intensities of the S_1 photoemission band (a) and of the A_1 photoemission band (b) at 50 K (squares) and at 300 K (circles) as a function of the oxygen exposure.

cent calculations of Kato and Uta,⁶ the A_1 and A_2 bands can be assigned to the hybridization of atomic orbitals between the Si substrate atoms and oxygen atoms issued from the dissociation of O_2 molecules and located either on top of a Si dimer, or into the Si back bonds. The A_1 band can alternatively be associated⁶ with an oxygen molecule weakly adsorbed on the Si surface. As it can be seen from Figs. 1(a) and 1(b), the oxygen adsorption on the clean silicon surface gradually reduces the intensities of the S_1 and S_2 bands.

The electron photoemission spectra of Fig. 1 are associated with oxygen exposures up to 0.5 L at 50 K and up to 4 L at 300 K. These maximum exposures correspond to a decrease of the S_1 band intensity by a factor 0.5 at both temperatures as can be seen from Fig. 2(a). The intensity of the S_1 band was reported rather than that of the S_2 band since the S_1 band intensity is not affected by the neighboring A_2 band. The intensity of the A_1 photoemission band as a function of the oxygen exposure is shown in Fig. 2(b). The slopes of the S_1 and A_1 band intensities in Fig. 2 are much higher at 50 K than at 300 K. This indicates that oxygen adsorption is more efficient at low temperature. Let us point out that, at both temperatures, the A_1 and A_2 band intensities increase regularly with the oxygen exposure.

B. Photon stimulated desorption of ions

Monitoring the A_1 and A_2 photoemission band intensities is a convenient way to study the oxygen content on the silicon surface,²³ but it cannot discriminate between different oxygen bonding configurations, due to the broadness of the bands. To access specific oxygen configurations, we have

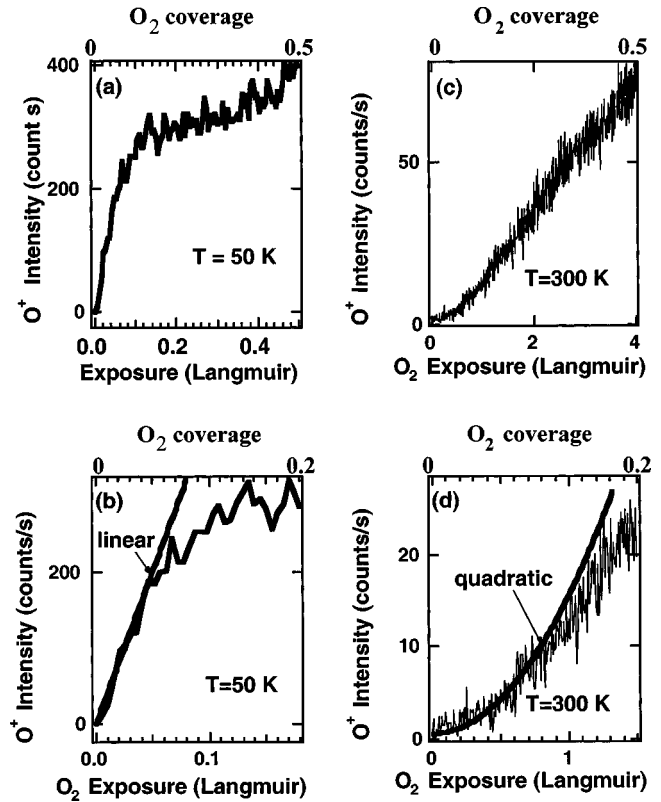


FIG. 3. *In situ* monitoring of the O^+ ion desorption yield as a function of O_2 exposure on the Si(100) 2×1 surface at 50 K [(a) and (b)] and 300 K [(c) and (d)]. The indicated O_2 coverage has been deduced from the decrease of the S_1 band in Fig. 2(a). The photon energy is 120 eV.

recorded the O^+ ion yield as a function of the oxygen exposure (see mode I described in Sec. II) and for a given exposure, as a function of the photon energy (see mode II in Sec. II). Monitoring the O^+ yield has an important advantage since only topmost oxygenated species are involved in the ion photodesorption process: this provides a high selectivity to the presence of very specific adsorption configurations. In Figs. 3(a) and 3(b) the O^+ desorption yield is shown as a function of oxygen exposure up to 0.45 L at low temperature ($T=50$ K) and up to 4 L at room temperature. The O^+ intensity has also been expressed in Fig. 3 as a function of the oxygen coverage. As seen in Fig. 2(a), the S_1 band intensity is approximately a linear decreasing function of the O_2 exposure. It follows that the oxygen coverage is also a linear function of the O_2 exposure. The oxygen coverage has been obtained from the reduction of the S_1 band in the photoemission spectra [see Fig. 2(a)]. It is clear from Fig. 4 that, for similar coverages, the O^+ desorption yield is much higher (by a factor 5 for a coverage of 0.5) at low temperature than at room temperature. This may be either due to different adsorption configurations at both temperatures or to some specific effect on the ion desorption process itself.²⁴ The two adsorption curves in Figs. 3(a) and 3(c) are obviously quite different. Oxygen adsorption at low temperature is characterized by a rapid and linear O^+ increase during the first 0.06 L, followed by a slow and nonlinear increase afterwards [Fig.

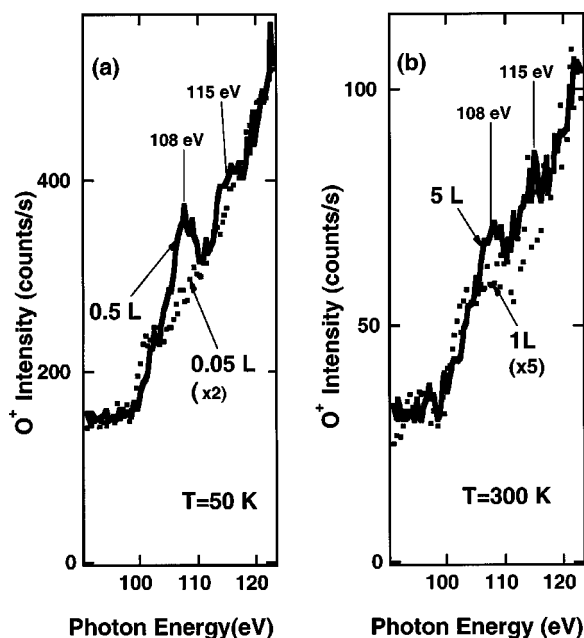


FIG. 4. O⁺ ion yield at 50 K (a) and 300 K (b) as a function of photon energy. The O⁺ spectra were recorded after a 0.05 and 0.5 L oxygen exposures at 50 K (a) and 1 and 5 L oxygen exposures at 300 K (b).

3(a)]. By contrast, at room temperature the O⁺ yield increases quadratically in the 0–1 L range [Fig. 3(c)]. We emphasize here that a linear increase of the O⁺ signal with oxygen exposure indicates that the O⁺ ion desorption is issued from a surface site produced by the adsorption of a single molecule whereas a quadratic increase indicates that O⁺ ion desorption originates from the adsorption of two oxygen molecules at the same surface site.²³ This is valid whatever the adsorbed molecule(s) stay intact as a molecule or dissociate upon adsorption. These results show that the initial oxygen molecules adsorb differently at 50 and 300 K: at 50 K, after adsorption of a single molecule there is at least one oxygen atom in the ad position, while at 300 K the two oxygen atoms of the molecule are in the backbonds. To get more insight into the adsorption configurations revealed by the presence of O⁺ photodesorbed ions, we recorded, in separate experiments, the photon-stimulated desorption spectra of O⁺ ions as a function of the photon energy (see mode II described in Sec. II) after a certain amount of oxygen has been adsorbed on the surface. Figures 4(a) and 4(b) show the O⁺ desorption yield as a function of the photon energy at 50 and 300 K, respectively. The room temperature data [Fig. 4(b)] have a too poor statistics to enable a comparison between low (1 L) and high (5 L) exposures. In the case of the low temperature adsorption [Fig. 4(a)] the PSD O⁺ spectra were recorded at two oxygen exposures: 0.05 L [in the linear part of the O⁺ yield versus exposure in Fig. 3(a)] and 0.5 L [in the nonlinear part of the O⁺ yield versus exposure in Fig. 3(a)]. These oxygen exposures were chosen such as to access the difference in the oxygen bonding (if it exists) throughout the exposure. As evidenced in Fig. 4(a), the two curves are quite different. Distinct resonances located at photon energies of 108 and 115 eV appear in the PSD O⁺ ion spectrum

recorded after the 0.5 L oxygen exposure, whereas only a step edge at about 100 eV is observed in the 0.05 L exposure spectrum.

C. Discussion

Let us first concentrate on the low temperature (50 K) results. In the low exposure range (<0.06 L), the O⁺ photo-desorption has evidenced a single adsorption configuration (adsorption of a single O₂ molecule at a given surface site) characterized by a nonresonant yield. This single adsorption configuration is not observed at 300 K [see Fig. 3(d)]. This means that a metastable species able to give rise to O⁺ photo-desorption with a nonresonant yield is formed by adsorption of a single oxygen molecule at 50 K. This metastable species is unstable during oxygen adsorption at 300 K, and may therefore be considered as a precursor of the molecular adsorption. Since it gives rise to O⁺ ion desorption, this precursor species is expected to have at least one oxygen atom in the ad position, that is to say on top of a silicon surface atom, according to our previous studies on the adsorption of O₂ on Si(111) 7×7 (Ref. 23). The fact that photodesorbed ion species originate preferentially from on top adsorption sites rather than from subsurface sites is an important feature of the ion photodesorption method. It is well known indeed that monovalent species such as fluorine and chlorine atoms desorb much more efficiently than divalent (oxygen) and trivalent (nitrogen) species. Monovalent species are expected to be adsorbed mainly on top positions, whereas divalent and trivalent species are expected to be adsorbed as subsurface species. This very high sensitivity of the ion desorption signal to species adsorbed on top position is one of the main advantages for using the ion desorption method to probe specific surface sites.

The exact nature of the oxygen precursor species is, however, difficult to deduce. The physisorbed O₂ molecules seem to be unstable on the silicon surface under our experimental conditions ($T=50$ K) since they were found to desorb already at about 35 K (Ref. 15). Thus the precursor species observed at 50 K should be a chemisorbed precursor. The question is whether the oxygen precursor is a weakly chemisorbed O₂ molecule or a dissociated O₂ molecule (one O atom in the ad position and the other one in the Si back bond). The UPS data cannot help to clarify the exact nature of the oxygen precursor: no characteristic band has been observed at low temperature and low exposure in the observed binding energy range from 0 up to 11 eV. As we did not observe any O₂⁺ photodesorption, we can argue that the precursor is not a chemisorbed molecule. Indeed, after NO adsorption on the Si(111) 7×7 surface at low temperature (50 K) and low exposure (0.5 L), NO⁺ ions have been observed to desorb.²⁵ However, here we cannot exclude that the precursor is a chemisorbed molecule even though we do not detect any O₂⁺ desorbed ion. Indeed such a chemisorbed molecule could well dissociate during the ion desorption process. Therefore, we cannot distinguish here between two possible configurations of the precursor, namely, a chemisorbed molecule or a dissociated molecule with an oxygen on top of the Si surface and the other one in the Si back bond. We note

that this result is apparently compatible with those of Seo *et al.*¹⁶ who observed an increase of the work-function when adsorbing O₂ at low temperature. Seo *et al.*¹⁶ proposed a chemisorbed molecule configuration for the precursor although the dissociated molecule configuration with an oxygen atom on top position would also fit well with their data. However, due to the different sensitivities of the ion desorption method used here and the work function method used by Seo *et al.*,¹⁶ it seems that the precursor species detected here are different from the metastable molecular species of Ref. 16. Indeed, at 50 K, we observed a saturation of the O⁺ intensity due to the precursor species at an oxygen exposure as low as 0.06 L, whereas the saturation of the work function change due to the precursors in Ref. 15 occurs at much higher oxygen exposures of 1 L. Similarly the existence of metastable oxygen species between 35 and 90 K has been inferred by Silvestre and Shaeyegan¹⁵ from high radiation electron energy loss spectroscopy and work function measurements. However, again only high oxygen exposures (5 L) regimes have been investigated in this latter work. The ion desorption method that we have used in the present work is a very surface sensitive method. It has enabled us to probe a very low oxygen exposure regime which is markedly different from high oxygen exposure regimes previously studied.^{15,16}

It is striking to note that the rapid increase of the O⁺ desorption yield at 50 K [Fig. 3(a)] saturates at an O₂ exposure of about 0.06 L, which has been found to correspond to an O₂ coverage of about 6%. This indicates that, in this low temperature regime, the oxygen sticking coefficient is unity. This percentage (6%) coincides with the mean value of proportion of type C defects, which are usually found on Si(100) 2×1 surfaces.²⁶ It follows that the initial oxygen adsorption most probably starts at type C defects,²⁷ as observed at room temperature,^{17,18} although the oxygen adsorption configurations are different at low temperature and room temperature. It is interesting to note that even though the O₂ molecules adsorb at defect sites, the S₁ and S₂ surface states intensities seem to have decreased already after an O₂ exposure of 0.05 L [Figs. 1(a) and 2(a)]. This is most probably due to the fact that the oxygen adsorption on the defects sites modifies the character of the neighboring dimers, which become metallic and therefore no longer contribute to the S₁ and S₂ bands.²⁸ When the oxygen exposure is higher than 0.06 L, the convex shape of the O⁺ ion yield [Fig. 3(a)] indicates that the ion desorption originates from the adsorption of two oxygen molecules adsorbed at the same surface site. Since the corresponding O⁺ yield as a function of the photon energy [Fig. 4(a)] shows the characteristic resonances at 108 and 115 eV, one can infer that these two molecules adsorption sites have a structure similar to the ones in silica as it has been observed in the case of the adsorption of O₂ on Si(111) 7×7 (Ref. 23).

As seen in Fig. 3, the O⁺ ion desorption is markedly different at 300 K as compared to 50 K. The convex ion yield

curve in Fig. 3(c) indicates that the ion desorption is issued from the adsorption of two oxygen molecules.²³ This result is very similar to what has been observed in the room temperature adsorption of oxygen on Si(111) 7×7 (Ref. 23). Therefore, like in this latter case, one can derive here that the adsorption of a single oxygen molecule on a given surface site is mainly dissociative with the two oxygen atoms being adsorbed into the silicon back bonds (no ion desorption) whereas the adsorption of a second oxygen molecule on the same site should produce at least one oxygen on top of the silicon atom (producing ion desorption). However, the oxygen adsorption on the Si(100) surface is somewhat different from that on the Si(111) surface. As previously mentioned, several STM studies of the oxidation of Si(100) 2×1 at room temperature^{17,18} have evidenced that the initial oxygen adsorption appears localized at defect sites, and particularly at the C-type defects. This was understood as follows. The Si(100) 2×1 surface has a semiconductive character and therefore the well-reconstructed areas of the surface are not reactive. On the contrary, the defects, and particularly the type-C defects, have a metallic character and therefore are easily oxidized. It has been further observed, by STM,^{17,18} that this initial oxidation modifies the neighbor Si dimers which in turn become reactive to oxygen and have a tendency to form a cluster. It follows that many different adsorption sites of oxygen most probably exist on the Si(100) surface at various oxygen exposures.

We note that our observation of an oxygen precursor on the Si(100) surface at low temperature is quite compatible with the metastable silanone intermediate observed at low temperature by infrared-absorption measurements.²⁰ However, the oxygen precursor is observed here at very low oxygen exposure (<0.06 L) whereas the metastable silanone intermediate²⁰ has been detected at a much higher oxygen exposure (15–80 L). Therefore, it may well be completely different oxidation sites observed in both experiments.

IV. CONCLUSION

Molecular oxygen adsorption on the clean Si(100) 2×1 surface has been compared at low temperature and room temperature in the low exposure regime. Valence band electron photoemission spectra recorded as a function of oxygen exposure show that the efficiency of the adsorption is much higher at low temperature than at 300 K. Ion photodesorption studies have evidenced the presence of an oxygen precursor configuration at 50 K, which does not exist at 300 K. The oxygen precursor at 50 K most probably results from the adsorption of an O₂ molecule on a type-C defect of the Si(100) 2×1 surface. It is considered that the O₂ molecule either weakly chemisorbs, or dissociates upon adsorption on the surface at 50 K with a penetration of only one O atom into the silicon back bonds, the other O atom being in the ad position. On the contrary, at 300 K, a more stable configuration is inferred where the O₂ molecule dissociates and both O atoms penetrate into silicon back bonds.

*Present address: Laboratoire des Collisions Atomiques et Moléculaires, Bât. 351, Université de Paris-Sud, 91405 Orsay, France.

- ¹M. Schulz, *Nature (London)* **399**, 729 (1999).
- ²D. A. Muller, T. Sorsch, S. Moccio, F. H. Baumann, K. Evans-Lutterodt, and G. Timp, *Nature (London)* **399**, 758 (1999).
- ³G. Timp *et al.*, in IEDM Technical Digest 615-618 (IEDM, San Francisco, 1998).
- ⁴T. Uchiyama and M. Tsukada, *Phys. Rev. B* **55**, 9356 (1997).
- ⁵B. B. Stefanov and K. Raghavachari, *Surf. Sci.* **389**, L1159 (1997).
- ⁶K. Kato, T. Uda, and K. Terakura, *Phys. Rev. Lett.* **80**, 2000 (1998); K. Kato and T. Uda, *Phys. Rev. B* **62**, 15 978 (2000).
- ⁷H. Watanabe, K. Kato, T. Uda, K. Fujita, and M. Ichikawa, *Phys. Rev. Lett.* **80**, 345 (1998).
- ⁸B. A. Ferguson, C. T. Reeves, and C. B. Mullins, *J. Chem. Phys.* **110**, 11 574 (1999).
- ⁹M. Suemitsu, Y. Enta, Y. Miyanishi, and N. Miyamoto, *Phys. Rev. Lett.* **82**, 2334 (1999).
- ¹⁰H. W. Yeom, H. Hamamatsu, Ohta, and R. I. G. Uhrberg, *Phys. Rev. B* **59**, R10 413 (1999).
- ¹¹H. W. Yeom and R. Uhrberg, *Jpn. J. Appl. Phys., Pt. 1* **39**, 4460 (2000).
- ¹²K. Nakajima, Y. Okazaki, and K. Kimura, *Phys. Rev. B* **63**, 113314 (2001).
- ¹³A. Estève, Y. J. Chabal, K. Raghavachari, M. K. Weldon, K. T. Queeney, and M. D. Rouhani, *J. Appl. Phys.* **90**, 6000 (2001).
- ¹⁴Y. Tu and J. Tersoff, *Phys. Rev. Lett.* **89**, 086102 (2002).
- ¹⁵C. Sylvestre and M. Shayegan, *Solid State Commun.* **77**, 735 (1991).
- ¹⁶J. M. Seo, K. J. Kim, H. W. Yeom, and Ch. Park, *J. Vac. Sci. Technol. A* **12**, 2255 (1994).
- ¹⁷M. Udagawa, Y. Umetani, H. Tanaka, M. Itoh, T. Uchiyama, Y. Watanabe, T. Yokotsuka, and I. Sumita, *Ultramicroscopy* **42-44**, 946 (1992).
- ¹⁸Ph. Avouris and D. Cahill, *Ultramicroscopy* **42-44**, 838 (1992).
- ¹⁹D. Cahill and Ph. Avouris, *Appl. Phys. Lett.* **60**, 326 (1992).
- ²⁰Y. J. Chabal, K. Raghavachari, X. Zhang, and E. Garfunkel, *Phys. Rev. B* **66**, 161315 (2002).
- ²¹K. Bobrov, G. Comtet, G. Dujardin, and L. Hellner, *Phys. Rev. Lett.* **86**, 2633 (2001).
- ²²F. Lutz, J. L. Bishoff, L. Kubler, and D. Bolmont, *Phys. Rev. B* **40**, 10 356 (1989).
- ²³G. Comtet, L. Hellner, G. Dujardin, and K. Bobrov, *Phys. Rev. B* **65**, 035315 (2002).
- ²⁴G. Comtet, G. Dujardin, and L. Hellner, *Surf. Sci.* **528**, 210 (2003).
- ²⁵L. Hellner, G. Comtet, M. J. Ramage, K. Bovrov, M. Carbone, and G. Dujardin, *J. Chem. Phys.* **119**, 515 (2003).
- ²⁶R. J. Hamers and U. K. Köhler, *J. Vac. Sci. Technol. A* **7**, 2854 (1989).
- ²⁷M. Nishizawa, T. Yasuda, S. Yamasaki, K. Miki, M. Shinohara, N. Kamakura, Y. Kimura, and M. Niwano, *Phys. Rev. B* **65**, 161302 (2002).
- ²⁸A. J. Mayne, F. Semond, G. Dujardin, and P. Soukiassian, *Phys. Rev. B* **57**, 15 108 (1998).